Civil and Sustainable Urban Engineering

Research Article
Volume 6(2), 2026, 410–426
https://doi.org/10.53623/csue.v6i2.1436

High-Damping Rubber Bearing Base-Isolation Performance under Different Seismic Hazard Levels

Indra Ariani*, Fachriza Noor Abdi, Muhammad Jazir Alkas, Masayu Widiastuti, Budi Haryanto, Heri Sutanto, Triana Sharly P. Arifin, Citra Anggita, Chalsi Mala Sari, Moch. Gaharu D. Devedo, Dharwati P. Sari

Department of Engineering, Mulawarman University, Jl. Sambaliung No. 9, Gunung Kelua Campus, Samarinda 75119, East Kalimantan, Indonesia

*Correspondence: indraariani@ft.unmul.ac.id

SUBMITTED: 22 September 2026; REVISED: 15 October 2026; ACCEPTED: 19 October 2026

ABSTRACT: Base isolation can reduce seismic forces transmitted to building superstructures, but its effectiveness depends on seismic hazard conditions, bearing properties, and structural response. This study compares the reported seismic responses of a reinforced-concrete hospital building with fixed-base and high-damping rubber bearing (HDRB) configurations under three Indonesian seismic hazard scenarios: Samarinda, Aceh, and Palu. Six analytical cases were evaluated using identical reported building geometries. The assessment considered base shear, floor displacement, interstory drift, and P–Delta stability. The reported base shear decreased from 4,902 to 3,754 kN in Samarinda, from 16,371 to 10,914 kN in Aceh, and from 16,997 to 11,331 kN in Palu, corresponding to reductions of 23.42%, 33.33%, and 33.34%, respectively. The isolated models generally exhibited greater absolute floor displacements than the fixed-base models. However, inconsistencies between the reported floor-displacement and interstory-drift values prevent a definitive assessment of drift compliance. Furthermore, the available information is insufficient to independently verify the HDRB constitutive model or determine story-level P–Delta stability coefficients. Although the results demonstrate reduced base shear across all three HDRB configurations, these reductions alone do not establish full compliance with seismic design codes or ensure the hospital's operational continuity following an earthquake. Further verification of site-specific seismic spectra, bearing properties, isolation displacement capacity, interstory drift, and second-order effects is necessary before the findings can support final engineering design decisions.

KEYWORDS: Base isolation; high-damping rubber bearing; seismic response; base shear; interstory drift; hospital building

1. Introduction

Hospitals are critical facilities that must maintain essential functions during and after major earthquakes. However, their seismic performance cannot be evaluated solely in terms of structural collapse prevention. Excessive floor accelerations, interstory deformations, damage to nonstructural components, and disruptions to utility systems can compromise hospital operations even when the primary structure remains intact. This challenge highlights the need

for seismic protection systems that reduce structural demands while maintaining acceptable deformation and serviceability performance. Recent studies on high-damping rubber bearing (HDRB)-isolated hospitals have demonstrated that base isolation does not necessarily guarantee operational continuity, particularly under near-fault ground motions that may induce excessive bearing displacement, pounding, vertical acceleration, or undesirable superstructure responses [1, 2].

High-damping rubber bearings provide horizontal flexibility and energy dissipation through the mechanical properties of their rubber layers. By increasing the effective vibration period and dissipating seismic energy, HDRB systems can reduce earthquake-induced forces transmitted to the superstructure. Nevertheless, their effectiveness depends on ground-motion characteristics, structural and isolation periods, bearing stiffness, damping properties, and available displacement capacity. Previous investigations have examined HDRB performance in reinforced-concrete buildings, hillside structures, and alternative isolation configurations, demonstrating the influence of structural characteristics and isolation parameters on seismic response [3–8].

Comparative studies of fixed-base and base-isolated structures have also considered soft-soil conditions, existing reinforced-concrete buildings, and different seismic loading scenarios [9–16]. Although these investigations generally demonstrate the potential of isolation systems to reduce seismic force demands, their findings cannot be directly generalized across buildings with different geometries, site conditions, bearing properties, and analytical assumptions. Furthermore, reduced base shear does not necessarily indicate lower absolute floor displacement, acceptable interstory drift, or adequate isolation-system stability. These differences highlight the importance of evaluating multiple seismic response parameters rather than relying on a single performance indicator.

An additional challenge arises when comparing structural responses across different seismic-hazard locations. Variations in response may reflect differences in spectral characteristics, soil classification, structural periods, damping, and ground-motion properties rather than seismic hazard intensity alone. Consequently, comparisons involving different buildings or isolation configurations may obscure the influence of location-specific seismic demands. Using a consistent building configuration provides a more controlled basis for evaluating these differences, although the resulting conclusions remain dependent on the adopted analytical assumptions.

Despite extensive research on seismic isolation, a research gap remains in the consistent comparison of fixed-base and HDRB-isolated responses for the same reinforced-concrete hospital building under the Samarinda, Aceh, and Palu seismic-hazard scenarios. Existing studies have primarily examined individual structural configurations, specific seismic conditions, or particular isolation parameters [3–16]. A comparative assessment using identical nominal building geometry and isolation-system assumptions can provide additional insight into how relative seismic response varies across these three scenarios.

The novelty of this study lies in applying a consistent comparative framework to evaluate the reported seismic responses of the same hospital building under three Indonesian seismic-hazard scenarios. By comparing fixed-base and HDRB-isolated configurations, the study examines variations in base-shear reduction and floor-displacement response while maintaining consistent nominal structural geometry. This approach provides a preliminary assessment of whether the relative effectiveness of HDRB isolation remains comparable across

different seismic demands. Rather than proposing a new isolation device or analytical formulation, the study emphasizes the importance of interpreting force reduction alongside deformation and stability requirements. In particular, previous research has demonstrated that excessive isolation displacement and nonlinear response may compromise seismic performance despite reductions in transmitted forces [1, 2, 17–20].

Accordingly, this study aims to evaluate and compare the reported seismic responses of fixed-base and HDRB-isolated reinforced-concrete hospital buildings under the Samarinda, Aceh, and Palu seismic-hazard scenarios. Specifically, the objectives are to (1) quantify differences in base shear between fixed-base and HDRB-isolated configurations; (2) examine the reported floor-displacement and interstory-drift responses; (3) evaluate variations in relative isolation performance across the three seismic scenarios; and (4) identify the additional analytical information required to verify bearing displacement capacity, interstory-drift compliance, and P–Delta stability in accordance with applicable Indonesian seismic design provisions [24]. The findings are expected to provide a comparative basis for assessing HDRB effectiveness while identifying critical considerations for the seismic design and performance evaluation of hospital buildings.

2. Materials and Method

2.1. Building Configuration and Analytical Cases.

The investigated structure, Mulya Medika Hospital, is a reinforced-concrete building measuring 78.4 × 36.0 m in plan and 25.53 m in height. Six analytical cases were considered, comprising fixed-base (FB) and high-damping rubber bearing (HDRB) base-isolated (BI) configurations under three seismic-hazard scenarios: Samarinda (S-FB, S-BI), Aceh (A-FB, A-BI), and Palu (P-FB, P-BI). The fixed-base models restrained horizontal translation at the base, whereas the isolated models incorporated HDRB elements to provide flexibility and energy dissipation. Consistent superstructure geometry, material properties, seismic mass, loading conditions, and analytical settings were assumed for comparison, with differences limited to support and isolation properties.Table 1 summarizes the building characteristics and analytical cases used to compare base shear, floor displacement, interstory drift, and P–Delta stability across the three seismic-hazard scenarios.

Table 1. Building Configuration and Analytical Comparison Framework.

Parameter	Description
Building	Mulya Medika Hospital
Plan dimensions	78.4 m × 36.0 m
Reported total height	25.53 m
Structural configurations	Fixed base and HDRB base isolation
Locations	Samarinda, Aceh, and Palu
Number of analytical cases	Six
Main response quantities	Base shear, floor displacement, interstory drift, and P–Delta stability
Comparison basis	Reported responses for the same nominal building configuration

Figure 1 illustrates the three-dimensional structural model used to represent the hospital building. The model provides the geometric basis for evaluating the fixed-base and HDRB-isolated configurations across the three seismic-hazard scenarios. Maintaining consistent

building geometry is important for distinguishing the influence of the isolation system from differences associated with structural dimensions or arrangements.

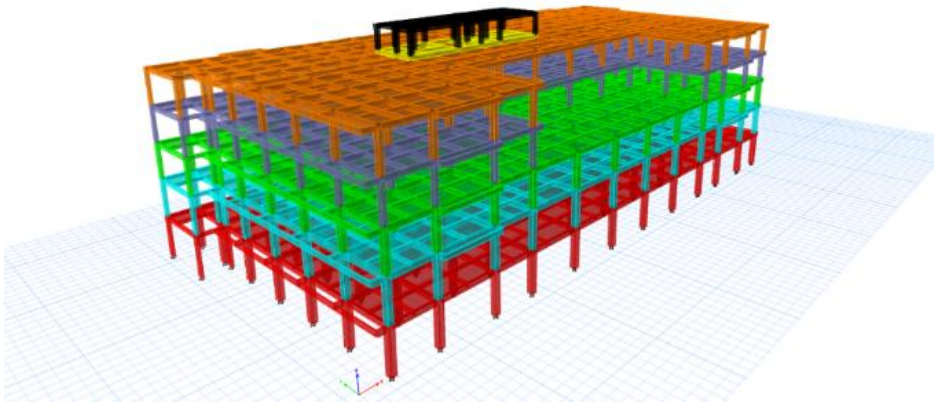


Figure 1. Structural Model of the Hospital Building.

The available documentation does not fully specify the structural member dimensions, concrete and reinforcement properties, seismic mass sources, diaphragm assumptions, foundation flexibility, modal periods, ground-motion records, or analytical software. These parameters are necessary for reproducing the simulations and verifying the consistency of the six analytical cases. Consequently, the present assessment is based on the reported structural configurations and response results, while detailed model verification requires the original analytical documentation.

2.2. Selection of Seismic-Hazard Scenarios and Spectral Parameters.

Samarinda, Aceh, and Palu were selected to represent contrasting seismic-hazard scenarios in Indonesia. Based on the supplied design parameters, Samarinda exhibits lower short-period spectral acceleration than Aceh and Palu, while Palu generally has the highest reported seismic demands. These locations were evaluated as comparative scenarios using the same nominal building configuration, without assuming identical soil conditions or ground-motion characteristics.

The reported seismic parameters are summarized in Table 2. the design short-period spectral acceleration increases from 0.192 g in Samarinda to 0.790 g in Aceh and 0.800 g in Palu. Similarly, the one-second design spectral acceleration increases from 0.273 g to 0.770 g and 0.800 g, respectively. These differences provide a basis for examining the influence of seismic-hazard scenarios on the relative performance of fixed-base and HDRB-isolated structures. The recalculated transition periods generally agree with the reported values, with minor differences attributable to rounding. However, the seismic parameters should be verified against the applicable hazard maps and site-specific design requirements before being used for final structural design. The design spectral transition periods are related to the short-period and one-second design spectral accelerations by Equations (1) and (2), respectively.

$$T_S = \frac{S_{D1}}{S_{DS}} \tag{1}$$

$$T_0 = 0.2T_S \tag{2}$$

Here, S_{DS} is the design spectral acceleration at short periods, S_{D1} is the design spectral acceleration at a period of one second, T_S is the transition period between the constant-acceleration and constant-velocity regions, and T_0 is the initial transition period.

Table 2. Reported seismic-hazard parameters for Samarinda, Aceh, and Palu

Parameter	Samarinda	Aceh	Palu
S_S (g)	0.12	1.4	1.5
S_1 (g)	0.097	0.55	0.6
S_{DS} (g)	0.192	0.79	0.8
S_{D1} (g)	0.273	0.77	0.8
T_0, reported (s)	0.285	0.2	0.2
T_S, reported (s)	1.424	0.98	1
T_S, recalculated (s)	1.422	0.98	1
T_0, recalculated (s)	0.284	0.2	0.2

Note: S_S and S_1 denote the mapped spectral accelerations at short periods and at a period of one second, respectively. S_{DS} and S_{D1} denote the corresponding design spectral accelerations. T_0 and T_S denote the transition periods. The reported values are supplied model inputs and have not been independently verified against official hazard maps.

The recalculated transition periods are consistent with the reported values after rounding. This arithmetic agreement does not independently validate the spectral accelerations. The values of S_S, S_1, S_{DS}, and S_{D1} must be checked against the official Indonesian response-spectrum resource, the adopted site classification, and the applicable design procedure [24, 25]. A common site class of SE was assumed in the original comparison. This assumption can be used as a controlled analytical variable, but it does not demonstrate that all three locations have the same soil profile. The justification for a common class should be supported by geotechnical information or explicitly described as a hypothetical comparison assumption. Final location-specific design requires a site classification supported by geotechnical investigation and the applicable code provisions. The response spectra must be generated from verified design parameters before a definitive graphical comparison can be reported. Because the supplied data do not include the original response-spectrum exports, the present manuscript does not claim that a validated three-location response-spectrum figure has been produced.

The design response spectra for Samarinda, Aceh, and Palu were developed using the reported seismic parameters and adopted site-class assumptions. Figure 2 compares the spectral acceleration demands across different structural periods, highlighting variations in seismic intensity and spectral characteristics among the three locations. Palu and Aceh exhibit substantially higher short-period spectral accelerations than Samarinda, indicating greater seismic demands on relatively stiff structures. At longer periods, the spectral response is governed by the corresponding transition periods and one-second design spectral accelerations, resulting in different rates of spectral acceleration reduction. These variations are particularly relevant to base-isolated buildings because HDRB systems increase the effective structural period, potentially shifting the response toward regions of lower spectral acceleration. However, the resulting force reduction depends on the effective isolation period, damping characteristics, and spectral shape rather than seismic intensity alone. Therefore, the comparison in Figure 2 provides a basis for interpreting differences in base shear and displacement between the fixed-base and HDRB-isolated configurations under the three seismic-hazard scenarios.

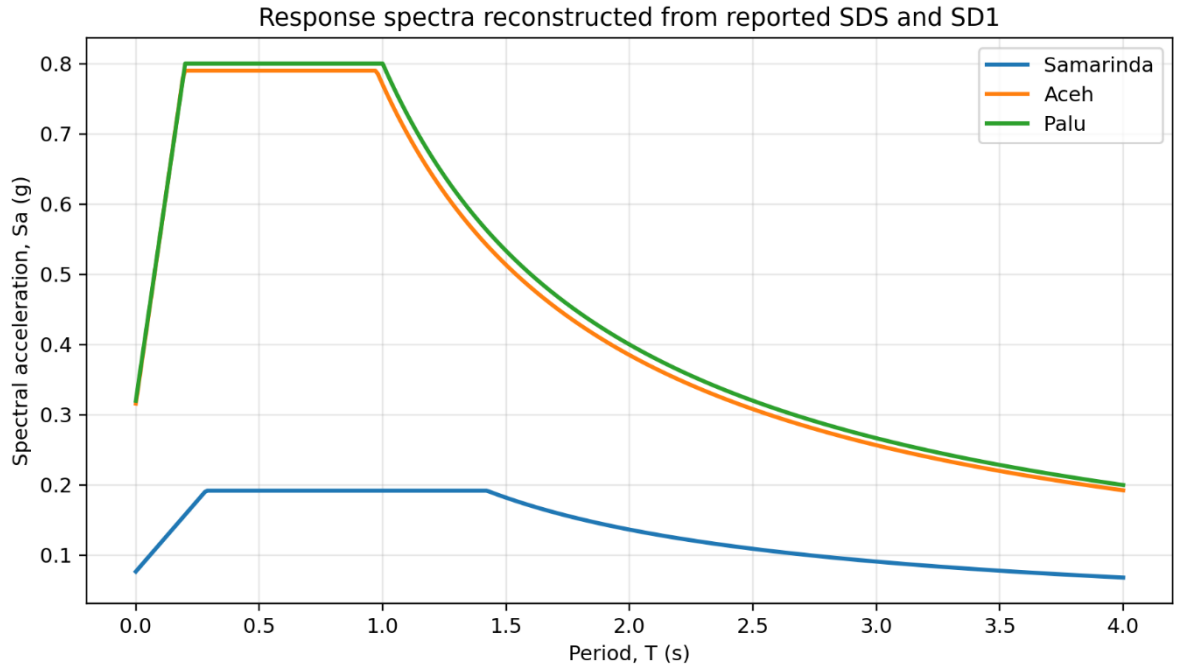


Figure 2. Design Response Spectra for the Three Seismic-Hazard Scenarios.

2.3. HDRB Properties and Modeling Assumptions.

The high-damping rubber bearing (HDRB) properties adopted in the analytical models are summarized in Table 3. The bearing has an outside diameter of 800 mm, a total rubber thickness of 197.2 mm, and an overall height of 322 mm. The nominal cross-sectional area of the circular bearing was calculated using Equation (3):

$$A = \frac{\pi D^2}{4} \tag{3}$$

where (A) is the nominal cross-sectional area (mm²) and (D) is the outside diameter (mm). Substituting the reported diameter gives an area of approximately 502,655 mm² (5,026.5 cm²), closely matching the reported effective area of 5,023 cm². The minor difference may reflect rounding or the manufacturer's definition of effective bearing area.

Table 3. Reported Geometric and Mechanical Properties of the HDRB

Parameter	Reported value	Unit
Outside diameter	800	mm
Effective area	5,023	cm²
Total rubber thickness	197.2	mm
Total bearing height	322	mm
Bearing weight	0.74	tonf
Compressive stiffness	2.490 x 10^6)	kN/m
Nominal column load	2,510	kN
Initial shear stiffness	(5.51 x 10^3)	kN/m
Post-yield shear stiffness	(0.551 x 10^3)	kN/m
Characteristic strength	42	kN
Equivalent shear stiffness	(0.764 x 10^3)	kN/m
Equivalent damping ratio	17	%

As shown in Table 3, the HDRB has a nominal column load of 2,510 kN and a reported compressive stiffness of 2.490×10^6 kN/m. Its horizontal mechanical response is characterized by an initial shear stiffness of 5.51×10^3 kN/m, which decreases to a post-yield stiffness of 0.551×10^3 kN/m. This reduction represents the intended nonlinear flexibility of the isolation system, allowing greater horizontal deformation while limiting the forces transmitted to the superstructure. The characteristic strength of 42 kN, equivalent shear stiffness of 0.764×10^3 kN/m, and equivalent damping ratio of 17% describe the reported energy-dissipation characteristics of the bearing. However, these parameters must be interpreted in relation to the displacement amplitude and loading conditions used to define them.

In the structural model, HDRB elements should reproduce the nonlinear horizontal force–displacement relationship through an appropriate constitutive formulation. For a bilinear representation, the initial and post-yield stiffnesses, characteristic strength, and equivalent damping properties must be consistently defined. The mechanical response may also vary with shear strain, loading frequency, temperature, and loading history, potentially affecting isolation displacement and seismic force reduction [17, 20].

The available documentation does not specify the analytical software, nonlinear link-element formulation, yield displacement, allowable shear strain, or experimental calibration procedure. Consequently, the values in Table 3 are treated as reported analytical inputs rather than independently validated bearing properties. Verification against manufacturer specifications or experimental hysteresis data is necessary to establish the reliability of the nonlinear model. Previous investigations of base-isolation systems provide relevant methodological references but cannot substitute for calibration of the specific HDRB configuration [3, 4, 9].

Figure 3 illustrates the geometric configuration and mechanical representation of the HDRB system incorporated into the isolated structural models. The bearing arrangement provides the physical basis for transferring vertical loads while accommodating horizontal deformation at the isolation level. Its layered rubber configuration contributes to horizontal flexibility, whereas the specified stiffness and damping characteristics govern the modeled seismic response. The figure should therefore be interpreted together with the mechanical parameters in Table 3, particularly the relationship between bearing geometry, horizontal stiffness, and energy dissipation.

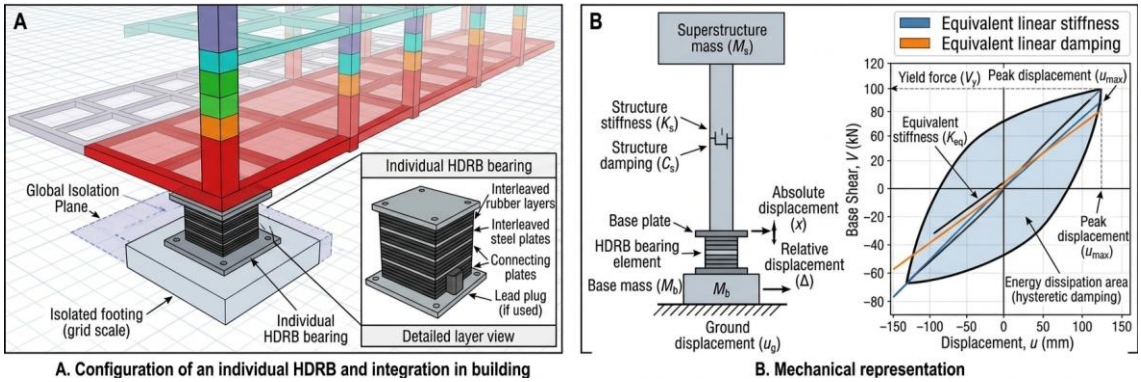


Figure 3. Configuration and Mechanical Representation of the HDRB System.

2.4. Base-Shear Reduction.

Base shear was evaluated to quantify the influence of high-damping rubber bearing (HDRB) isolation on the seismic force transmitted to the building superstructure. The percentage reduction was determined by comparing the reported base shear of each fixed-base model with that of its corresponding HDRB-isolated configuration using Equation (4):

$$R_V = \frac{V_{FB} - V_{BI}}{V_{FB}} x100\% \quad (4)$$

where R_V is the percentage reduction in base shear, V_{FB} is the base shear of the fixed-base model (kN), and V_{BI} is the base shear of the HDRB-isolated model (kN). A positive R_V indicates a reduction in seismic force demand following the introduction of base isolation, whereas a negative value indicates an increase.

The calculation was applied separately to the Samarinda, Aceh, and Palu scenarios to evaluate the relative effectiveness of HDRB isolation under different seismic demands. This comparison provides a quantitative measure of force reduction but does not independently establish overall seismic performance. Its validity also depends on the consistency of structural mass, damping assumptions, seismic load combinations, response-spectrum scaling, and analytical procedures between corresponding models. These conditions require confirmation against the original analytical documentation.

2.5. Floor Displacement and Interstory Drift.

Floor displacement and interstory drift were examined to evaluate the deformation response of the fixed-base and HDRB-isolated configurations. Floor displacement represents the lateral movement of a structural level relative to the selected global reference, whereas interstory drift describes the relative displacement between adjacent floors. These parameters provide complementary information because larger absolute floor displacements do not necessarily correspond to greater interstory deformation, particularly in base-isolated structures.
The interstory displacement was calculated using Equation (5) and the corresponding interstory drift ratio was determined using Equation (6):

$$\Delta_i = u_i - u_{i-1} \quad (5)$$

$$\gamma_i = \frac{\Delta_i}{h_i} \quad (6)$$

where Δ_i is the relative lateral displacement between adjacent floors, u_i and u_{i-1} are the lateral displacements of the upper and lower floors, respectively, (h_i) is the story height, and γ_i is the dimensionless interstory drift ratio. Consistent units were required for displacement and story height, while the drift ratio could also be expressed as a percentage.

The reported displacement and drift values were examined for internal consistency by comparing interstory displacement with the differences between adjacent floor displacements. Several reported drift values did not correspond to these differences, suggesting possible inconsistencies in data extraction, floor identification, or analytical output interpretation. Consequently, the reported drift results were retained for comparative discussion but were not considered independently verified for seismic-code compliance. Confirmation requires the original analysis outputs, governing load combinations, and floor-level definitions.

2.6. P–Delta Stability Assessment.

P–Delta effects represent second-order structural responses arising when gravity loads act through a laterally displaced building configuration. These effects can amplify lateral deformation and internal forces, particularly when structural flexibility increases. Their evaluation is therefore important for both fixed-base and HDRB-isolated buildings, although the isolation system may alter the distribution of lateral displacement and seismic force demand. The story stability coefficient was evaluated with reference to SNI 1726:2019 [24], as expressed in Equation (7):

$$\theta_i = \frac{P_x \Delta_x I_e}{V_x h_{sx} C_d} \tag{7}$$

Where P_x is the total vertical design load at and above level x, Δ_x is the design story drift, I_e is the seismic importance factor, V_x is the story shear between levels x and $x-1$, h_{sx} is the story height, and C_d is the deflection amplification factor.

The maximum permitted stability coefficient is given by Equation (8).

$$\theta_{max} = \frac{0.5}{\beta_{cd}} \leq 0.25 \tag{8}$$

Where β is the ratio of shear demand to shear capacity between the two levels. Under the applicable provisions, a stability coefficient above 0.10 requires explicit consideration of second-order effects under the conditions specified in the standard. The maximum permitted value depends on β and cd; 0.10 is not a universal maximum allowable stability coefficient [24].

A value of approximately 0.0909 can be obtained from 0.5 / 5.5 only if β = 1.0 and cd = 5.5. These assumptions must be verified for the structural system under consideration. Because the required story-level gravity loads, shears, heights, and verified design drifts were not supplied, this study does not report unverified P–Delta coefficients or assert that a particular floor exceeds the stability limit.

3. Results and Discussion

3.1. Base-shear comparison.

The seismic base-shear responses of the fixed-base and HDRB-isolated configurations were compared under the three seismic-hazard scenarios. The reported base-shear values and percentage reductions calculated using Equation (4) are presented in Table 4. This comparison evaluates the effectiveness of the isolation system in reducing the lateral seismic forces transmitted to the building superstructure.

Table 4. Comparison of Reported Base Shear for Fixed-Base and HDRB-Isolated Models.

Location	Fixed base (kN)	HDRB-isolated (kN)	Difference (kN)	Reduction (%)
Samarinda	4,902	3,754	1,148	23.42
Aceh	16,371	10,914	5,457	33.33
Palu	16,997	11,331	5,666	33.34

As shown in Table 4, the HDRB-isolated configurations consistently exhibited lower base shear than their fixed-base counterparts. In Samarinda, base shear decreased from 4,902

to 3,754 kN, representing a reduction of 23.42%. Greater absolute reductions were observed in Aceh and Palu, where base shear decreased by 5,457 and 5,666 kN, respectively. The corresponding percentage reductions were 33.33% and 33.34%, indicating nearly identical relative force reductions in these two scenarios. These findings demonstrate that the introduction of HDRB isolation was associated with reduced seismic force demand across all three analytical cases.

The differences in reduction percentages suggest that the effectiveness of base isolation is influenced by the characteristics of the seismic input. Samarinda exhibited a reduction approximately 10 percentage points lower than those observed in Aceh and Palu. However, this variation cannot be attributed solely to seismic-hazard intensity because the structural response also depends on the shape of the design response spectrum, effective structural period, isolation stiffness, and damping characteristics. In particular, the increased flexibility introduced by HDRB isolation may shift the effective vibration period toward a region of lower spectral acceleration, thereby reducing the seismic forces transmitted to the superstructure. The magnitude of this reduction depends on the relationship between the isolated structural period and the corresponding design spectrum.

The observed reductions are consistent with the fundamental mechanism of base isolation, which limits seismic force transmission through increased horizontal flexibility and energy dissipation. Similar force-reduction behavior has been discussed in previous investigations of HDRB and other isolation systems [3,4,9,10]. Nevertheless, the present results should be interpreted within the specific building configuration and seismic scenarios investigated. Differences in structural geometry, isolation properties, ground conditions, and analytical procedures prevent direct generalization of the calculated reductions to other buildings. Furthermore, lower base shear does not necessarily indicate improved performance in every response parameter, particularly because isolation may increase absolute displacement and impose additional deformation demands on the bearings. Figure 4 provides a graphical comparison of the base-shear responses for the fixed-base and HDRB-isolated configurations.

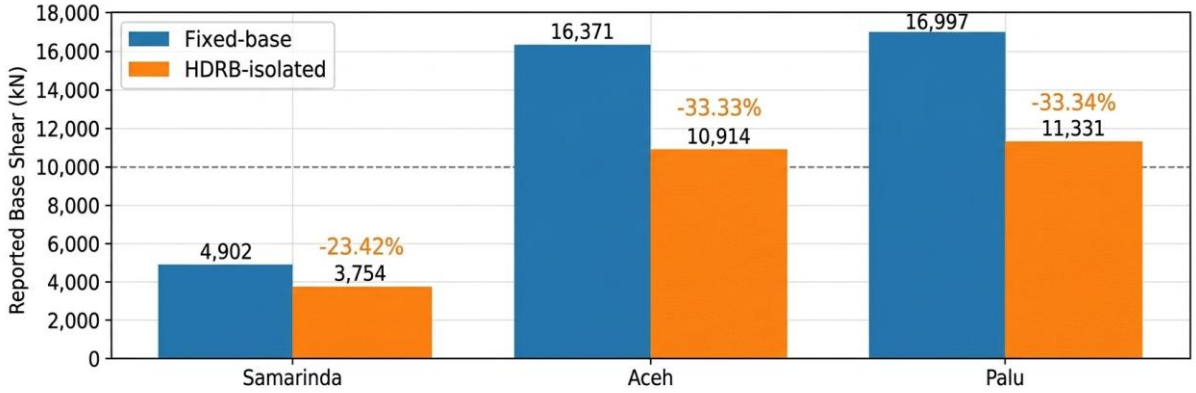


Figure 4. Comparison of Reported Base Shear for Fixed-Base and HDRB-Isolated Configurations.

The figure highlights the substantially higher seismic force demands in Aceh and Palu compared with Samarinda, reflecting the differences in their adopted seismic-hazard parameters. Although the isolated configurations maintain lower base shear in all three locations, the absolute forces remain considerably greater in Aceh and Palu. This indicates that HDRB isolation reduces the reported seismic demand without eliminating the influence of regional hazard characteristics. The relatively similar reductions in Aceh and Palu also suggest comparable force-reduction behavior under their respective analytical conditions. When interpreted together with Table 4, Figure 4 illustrates both the absolute

differences in seismic forces and the relative effectiveness of the isolation system across the three scenarios.

3.2. Floor-Displacement Response.

The lateral displacement responses of the fixed-base and HDRB-isolated configurations were evaluated in the X and Y directions to examine the influence of base isolation on structural deformation. The reported floor displacements for the three seismic-hazard scenarios are presented in Tables 5 and 6, respectively. The analysis considers seven structural levels, comprising Roof Lift, Attic, Floors 5 to 2, and Base. The results provide a comparative assessment of absolute lateral displacement under different seismic demands.

Table 5. Reported Floor Displacement in the X direction (mm)

Level	S-FB	S-BI	A-FB	A-BI	P-FB	P-BI
Roof Lift	19.24	30.77	59.36	89	61.44	97.02
Attic	18.47	30.33	67.67	91.77	67.57	100.04
Floor 5	16.37	29.4	59.96	89.08	59.87	97.11
Floor 4	12.95	28.13	47.67	84.85	47.6	92.5
Floor 3	8.67	26.19	32.1	79.86	32.05	87.06
Floor 2	3.43	23.44	13.51	72.63	13.54	79.18
Base	0	20.51	0	64.46	0	70.27

Table 6. Reported Floor Displacement in the Y direction (mm)

Level	S-FB	S-BI	A-FB	A-BI	P-FB	P-BI
Roof Lift	27.76	33.22	84.89	103.64	83.51	112.98
Attic	26.93	32.04	98.25	118.61	85.14	129.29
Floor 5	23.93	30.93	87.29	114.79	75.75	125.14
Floor 4	18.63	29.11	67.83	107.82	58.91	117.55
Floor 3	12.23	26.71	44.55	98.72	38.69	107.62
Floor 2	4.69	23.37	17.09	86.12	15.42	93.89
Base	0	20.05	0	72.14	0	78.64

Tables 5 and 6 generally show larger reported absolute displacements in the isolated cases than in the corresponding fixed-base cases. This pattern may be consistent with the intended behavior of base isolation, in which greater lateral movement is accommodated at the isolation interface while the force transmitted to the superstructure is reduced. The reported isolated-model base displacements are nonzero. Their interpretation depends on the coordinate reference and output definition used in the analysis. They may represent isolation-level movement or global displacement rather than deformation of the superstructure alone. The reference point and locations at which displacements were extracted must therefore be documented. The displacement profiles are also not consistently monotonic with the stated level order. For example, the Samarinda fixed-base X-direction displacement decreases from 19.24 mm at Roof Lift to 18.47 mm at Attic, whereas the Aceh fixed-base X-direction displacement increases from 59.36 mm to 67.67 mm between those levels. These patterns may reflect modal response, inconsistent level labeling, output selection, or transcription errors. The original analysis tables must be checked before definitive displacement profiles or drift ratios are calculated.

The higher reported displacement of the isolated models is important for design. It must be checked against bearing deformation capacity, seismic separation gaps, potential pounding, and the flexibility of utility connections. Research on isolated hospitals has shown that excessive isolation displacement and pounding can compromise performance even when the isolation system reduces force transmission [1]. Consequently, the displacement results cannot be interpreted as evidence of either satisfactory or unsatisfactory isolation performance without verified displacement demands and capacity limits. The reported floor-displacement profiles in the X and Y directions are compared in Figure 5 for the fixed-base and HDRB-isolated configurations. The profiles are intended to illustrate the distribution of lateral displacement over the building height. Their interpretation depends on confirmation of the floor labels, displacement reference, and isolation-level output definitions used in the original analysis.

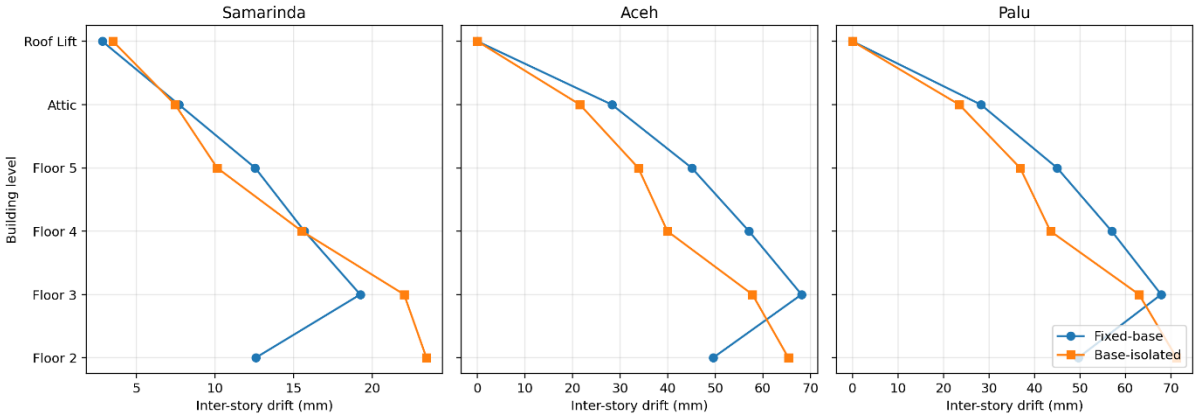


Figure 5. Reported Floor-Displacement Profiles in the X and Y Directions.

3.3. Interstory drift and structural deformation.

Interstory drift was examined to assess the relative lateral deformation between adjacent floors in the fixed-base and HDRB-isolated configurations. The reported drift values in the X and Y directions are presented in Tables 7 and 8, respectively. These parameters are important for evaluating structural deformation and potential damage to structural and nonstructural components under seismic loading. As shown in Table 7, the reported X-direction drift values exhibit different trends across the three seismic scenarios. In Aceh, the HDRB-isolated configuration generally shows lower reported values than the fixed-base model from the Attic to Floor 3, whereas the opposite occurs at Floor 2. A similar pattern is observed in Palu, where the isolated model exhibits lower values at several upper levels but higher values at Floor 2. Samarinda shows smaller differences between configurations, with the isolated model recording higher values at Floors 2 and 3. These variations suggest that the reported deformation response is not uniformly reduced by base isolation at every level. However, the values require verification before they can be interpreted as actual interstory drift demands. Table 8 indicates that the reported Y-direction drift values are generally greater than those in the X direction, particularly under the Aceh and Palu scenarios. In Aceh, the isolated model shows lower values at the Attic, Floor 5, and Floor 4, but higher values at Floor 2. In Palu, the isolated configuration records higher values at Floors 2–4, reaching 122.00 mm at Floor 2 compared with 56.53 mm for the fixed-base model. These results indicate substantial differences in the reported deformation patterns between structural configurations and loading

directions. Nevertheless, the apparent increases or decreases cannot be attributed conclusively to HDRB behavior without confirming the underlying drift calculations.

Table 7. Reported Interstory Drift in the X Direction (unit reported as mm)

Level	S-FB	S-BI	A-FB	A-BI	P-FB	P-BI
Roof Lift	2.83	3.51	0	0	0	0
Attic	7.7	7.46	28.27	21.55	28.23	23.48
Floor 5	12.55	10.13	45.06	33.82	45	36.86
Floor 4	15.68	15.52	57.1	39.94	57.01	43.54
Floor 3	19.23	22.02	68.14	57.82	67.88	63.02
Floor 2	12.58	23.44	49.54	65.38	49.64	71.28

Table 8. Reported Interstory Drift in the Y Direction (unit reported as mm)

Level	S-FB	S-BI	A-FB	A-BI	P-FB	P-BI
Roof Lift	3.01	9.42	0	0	0	0
Attic	11	8.86	40.19	30.54	34.46	33.25
Floor 5	19.44	14.56	71.38	55.74	61.75	60.73
Floor 4	23.46	19.23	85.36	72.82	74.14	79.38
Floor 3	27.66	26.74	100.7	100.8	85.32	109.9
Floor 2	17.19	26.58	62.67	111.9	56.53	122

An internal consistency check revealed discrepancies between the reported drift values and the floor displacements presented in Tables 5 and 6. For example, the Aceh fixed-base Y-direction displacements at Roof Lift and Attic are 84.89 and 98.25 mm, respectively, giving an absolute difference of 13.36 mm, whereas Table 8 reports zero drift at Roof Lift. Although peak floor displacements from different response-spectrum combinations cannot necessarily be subtracted to obtain design drift, this inconsistency highlights the need to verify the output definitions and calculation procedures. Accurate assessment requires consistent adjacent-level mapping, appropriate seismic load combinations, and verified story heights. Figure 6 presents the interstory-drift profiles in the X and Y directions to illustrate the reported distribution of lateral deformation along the building height. The profiles provide a visual comparison of the fixed-base and HDRB-isolated configurations, particularly the differences observed at intermediate and lower levels. However, because the tabulated drift values have not been reconciled with the original analytical outputs, the figure should be regarded as a preliminary representation rather than a verified design-level assessment.

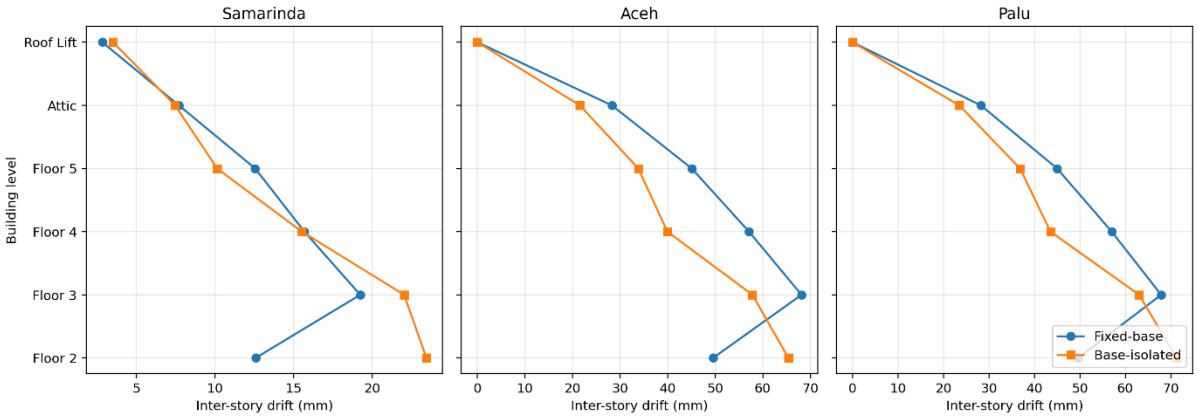


Figure 6. Verified Interstory-Drift Profiles in the X and Y Directions.

3.4. P–Delta stability and structural-design implications.

The supplied dataset does not provide all the story-level parameters required to calculate the P–Delta stability coefficient for each floor and seismic-hazard scenario. These parameters include vertical design loads, story shears, story heights, verified design drifts, the seismic importance factor, and the deflection amplification factor. Furthermore, inconsistencies in the reported interstory-drift values prevent reliable independent verification of second-order effects. The proposed stability limit of 0.0909 should not be considered universally applicable because it is obtained from Equation (8) only when (\beta = 1.0) and (C_d = 5.5). The appropriate stability limit must be determined according to the structural system and the relevant provisions of SNI 1726:2019 [24]. Without complete story-level data, it is not possible to determine whether the stability coefficients for the Aceh and Palu scenarios exceed the applicable limits or to identify the critical story.

Lower stories may be particularly important in P–Delta assessments because they typically support greater cumulative gravity loads. However, the maximum stability coefficient cannot be determined from absolute floor displacement alone, as it depends on the combined effects of vertical load, story shear, story height, and design drift. A reliable assessment therefore requires story-by-story calculations, comparison with the applicable stability limits, and consideration of second-order analysis or amplification where necessary. From a structural design perspective, the observed base-shear reductions do not necessarily indicate satisfactory performance across all seismic response parameters. Although HDRB isolation can reduce the lateral forces transmitted to the superstructure, it may increase displacement demands at the isolation interface. Therefore, the superstructure must be evaluated for interstory drift and second-order effects, while the isolation system requires verification of axial-load capacity, shear deformation, stability, and displacement capacity. For hospital buildings, adequate seismic separation gaps and flexible utility connections are also essential to reduce the risk of damage and maintain post-earthquake functionality.

3.5. Overall Interpretation and Limitations.

The results demonstrate consistent reductions in reported base shear following the introduction of HDRB isolation across the three seismic-hazard scenarios. These reductions are reproducible from the supplied analytical values and indicate the potential effectiveness of base isolation in reducing seismic force demand. However, the reliability of the remaining response parameters requires further verification. Several limitations should be considered when interpreting the findings. First, the seismic-hazard parameters have not been independently verified against official hazard maps or site-specific geotechnical data. Second, the reported HDRB properties have not been confirmed against manufacturer specifications, and the nonlinear link-element formulation lacks sufficient documentation to verify its calibration. Third, inconsistencies between the displacement and interstory-drift results prevent reliable assessment of drift compliance. Finally, the absence of complete story-level data limits the evaluation of P–Delta stability and associated second-order effects.

Consequently, the findings should be regarded as a preliminary comparison of the reported seismic responses rather than a comprehensive verification of structural performance. Although HDRB isolation demonstrates potential benefits in reducing base shear, the available evidence is insufficient to establish full compliance with seismic design standards, validate

bearing performance experimentally, or confirm post-earthquake hospital operational continuity. Further verification of seismic inputs, isolation properties, structural deformation, and stability requirements is necessary before the results can support final engineering design decisions.

4. Conclusions

This study evaluated the reported seismic responses of a reinforced-concrete hospital building with fixed-base and high-damping rubber bearing (HDRB) isolation configurations under three Indonesian seismic-hazard scenarios: Samarinda, Aceh, and Palu. The HDRB-isolated models consistently exhibited lower base shear, with reductions of 23.42%, 33.33%, and 33.34%, respectively. These findings indicate the potential effectiveness of HDRB isolation in reducing seismic forces transmitted to the superstructure. However, the isolated configurations generally exhibited greater absolute floor displacements, highlighting the importance of evaluating bearing deformation capacity, seismic separation gaps, potential pounding, and utility-connection flexibility. Inconsistencies between the reported floor-displacement and interstory-drift values prevented reliable verification of drift compliance. Similarly, the available story-level data were insufficient to calculate P–Delta stability coefficients or establish compliance with the applicable stability limits. The reported HDRB properties, particularly the compressive stiffness and nonlinear link-element formulation, also require confirmation against manufacturer specifications or experimental measurements. The principal contribution of this study is the comparative assessment of the same nominal hospital building under three contrasting seismic-hazard scenarios, demonstrating consistent base-shear reductions while identifying critical limitations in the available structural response data. Future investigations should verify site-specific seismic parameters, calibrate the HDRB mechanical model, reconcile displacement and drift outputs, and conduct comprehensive story-by-story stability assessments. Additional evaluations of isolation displacement capacity and nonstructural component performance are necessary to establish the practical suitability of the proposed system. Overall, the findings support the preliminary effectiveness of HDRB isolation but do not establish full seismic-code compliance or guarantee post-earthquake hospital operational continuity.

Author Contribution

Conceptualization: Indra Ariani, Fachriza Noor Abdi, Muhammad Jazir Alkas; Methodology: Indra Ariani, Masayu Widiastuti, Budi Haryanto; Data Collection: Heri Sutanto, Triana Sharly P. Arifin, Citra Anggita; Data Analysis: Indra Ariani, Fachriza Noor Abdi, Chalsi Mala Sari, Moch. Gaharu D. Devedo; Original Draft: Indra Ariani, Fachriza Noor Abdi; Review and Editing: Muhammad Jazir Alkas, Masayu Widiastuti, Budi Haryanto, Dharwati P. Sari; Resources: All authors, as applicable.

Data Availability Statement

Conceptualization: Indra Ariani, Fachriza Noor Abdi, Muhammad Jazir Alkas; Methodology: Indra Ariani, Masayu Widiastuti, Budi Haryanto; Data Collection: Heri Sutanto, Triana Sharly P. Arifin, Citra Anggita; Data Analysis: Indra Ariani, Fachriza Noor Abdi, Chalsi Mala Sari, Moch. Gaharu D. Devedo; Original Draft: Indra Ariani, Fachriza Noor Abdi; Review and

Editing: Muhammad Jazir Alkas, Masayu Widiastuti, Budi Haryanto, Dharwati P. Sari; Resources: All authors, as applicable.

Data Availability Statement

The numerical data are presented in the manuscript. Supporting structural models, analytical outputs, seismic spectra, and bearing specifications may be obtained from the corresponding author upon reasonable request, subject to availability and applicable restrictions.

Competing Interest

All authors should disclose any financial, personal, or professional relationships that might influence or appear to influence their research.

References

[1] Gallardo, J.A.; Chacón, M.F.; Muñoz, J.P.; et al. (2026). Earthquake response sensitivity of HDRB base-isolated hospitals to the crustal San Ramón Fault in Santiago, Chile. *Earthquake Engineering & Structural Dynamics*, *55*, 1631–1654. https://doi.org/10.1002/eqe.70154.

[2] Giuliani, G.; Sgobba, S.; Micozzi, F.; et al. (2026). Combined vertical and horizontal components of near-source earthquakes and impact on base-isolated structures. *Earthquake Engineering & Structural Dynamics*, *55*, 781–803. https://doi.org/10.1002/eqe.70109.

[3] Wahab, A.G.; Tao, Z.; Li, H.; Rasa, A.Y.; Huma, T.; Liang, Y. (2025). Dynamic simulation and seismic analysis of hillside RC buildings isolated by high-damping rubber bearings. *Infrastructures*, *10*, 239. https://doi.org/10.3390/infrastructures10090239.

[4] Chen, P.; Lu, Y.; Wang, B.; Zhuang, P.; Dai, K. (2025). Enhancing seismic resilience in base-isolated structures: A performance-based comparison of HDRB and LRB isolation systems. *Engineering Structures*, *342*, 120945. https://doi.org/10.1016/j.engstruct.2025.120945.

[5] Patel, D.; Kumar, R. (2026). Dynamic analysis of RC building in seismic zone V of India using base isolation. In Sustainable Materials and Technologies under Climate Change Scenario; Lecture Notes in Civil Engineering, Vol. 631; Springer: Singapore. https://doi.org/10.1007/978-981-96-5898-5_26.

[6] Adiastuti, R.; Wibowo, D.; Kartikasari, M. (2025). Performance evaluation of seismic base isolation systems in multi-storey structures located in high seismic zones. *International Journal of Structural Design and Engineering*, *6*, 24–29. https://doi.org/10.22271/27078280.

[7] Khofifah, N.; Habieb, A.B. (2026). Seismic performance enhancement of a reinforced concrete building using an RB-HDRC base isolation system. *G-Tech: Jurnal Teknologi Terapan*, *10*, 753–763. https://doi.org/10.70609/g-tech.v10i2.9398.

[8] Wahab, A.; Zhong, T. (2026). Seismic performance and energy dissipation of hillside reinforced concrete buildings isolated by high-damping rubber bearings: A DHI model-based study. *Innovative Infrastructure Solutions*, *11*, 53. https://doi.org/10.1007/s41062-025-02443-7.

[9] Yanik, A.; Okuroğlu, D. (2026). Comparative seismic performance of LRB and HDRB systems in reinforced concrete buildings. *Asian Journal of Civil Engineering*, *27*, 4275–4283. https://doi.org/10.1007/s42107-026-01722-7.

[10] Maulida, A.S.M.; Umniati, B.S.; Sulton, M.; Maulidani, A.A. (2025). Performance based design: Performance analysis on fixed base structure and structures with high damping rubber bearing (HDRB). *Bentang: Jurnal Teoritis dan Terapan Bidang Rekayasa Sipil*, *13*, 11–22. https://doi.org/10.33558/bentang.v13i1.10112.

[11] Salih, A.M.; Mohammad Ali, S.R.; Abdullah, T.A.; et al. (2026). Hybrid base isolation systems in earthquake engineering: Classification, experimental and analytical insights, and performance

assessment. *Asian Journal of Civil Engineering*, *27*, 4701–4713. https://doi.org/10.1007/s42107-026-01703-w.

[12] Gudainiyan, J.; Gupta, P.K.; Gupta, N. (2025). Effect of time period variation of HDRB on the response of a base-isolated building under near field earthquake. In Advances in Materials and Manufacturing; Lecture Notes in Mechanical Engineering; Springer: Singapore. https://doi.org/10.1007/978-981-96-7659-0_63.

[13] Misdi, M.; Hamzah, A. (2025). Time history analysis pada struktur bangunan yang menggunakan base isolator. *Jurnal Al Ulum LPPM Universitas Al Washliyah Medan*, *13*, 82–88. https://doi.org/10.47662/alulum.v13i1.874.

[14] Firmansyah, M.F.; Habieb, A.B.; Faimun, F. (2025). A study on the effects of implementing base isolation system for existing RC buildings on soft soil. *Journal of Civil Engineering*, *40*, 12–19. https://doi.org/10.12962/j20861206.v40i1.19925.

[15] Narjabadifam, P.; Mollaei, S.; Noroozinejad Farsangi, E.; Babaei, M.; Mousavi, N. (2024). Comparative probability-based seismic safety assessment of base-isolated buildings: A case study. *Advances in Civil and Architectural Engineering*, *15*. https://doi.org/10.13167/2024.28.3.

[16] Al-Sharief, M.O.; Al-Shaier, M.M. (2026). Study of seismic isolation in reinforced concrete buildings: Practical application and structural behavior. *Albahit Journal of Applied Sciences*, *5*. https://doi.org/10.65419/albahit.v5i2.141.

[17] Guo, F.; Cheng, L.; Liu, Y.; Meng, W.; Luo, T. (2026). Seismic performance assessment of isolated structures in cold regions: A rate-dependent large-strain model for HDRBs. *Structural Control and Health Monitoring*, *[volume]*, 8034720. https://doi.org/10.1155/stc/8034720.

[18] Mazza, F.; Braile, A.; Labernarda, R. (2026). Impact of the vertical component of near-fault earthquakes on the nonlinear response of RC structures with horizontal and vertical base-isolation. *Procedia Structural Integrity*, *78*, 33–40.

[19] Xu, G.; Guo, T.; Ni, X.-Y.; Zhi, G.-L.; Zhang, H.-Y.; Dang, L.-J. (2026). Breakthroughs in seismic isolation technologies for engineering structures. *International Journal of Structural Stability and Dynamics*, *26*, 2650062. https://doi.org/10.1142/S0219455426500628.

[20] Ragni, L.; Micozzi, F.; Dall'Asta, A. (2025). Long-term viscous effects of in-field tests on HDRBs-based seismic isolation systems. *Engineering Structures*, *[volume]*, 120647. https://doi.org/10.1016/j.engstruct.2025.120647.

[21] Yanto, D.; Tavio; Jusuf, A.H. (2025). Engineering assessment of earthquake resistant building code based on seismic load responses. *Advance Sustainable Science, Engineering and Technology*, *8*, 0260102. https://doi.org/10.26877/asset.v8i1.2400.

[22] Naiel, A.; Hanna, N.; Lotfy, I. (2025). Assessing seismic performance of mid-rise reinforced concrete buildings using fragility curves. *Innovative Infrastructure Solutions*, *10*. https://doi.org/10.1007/s41062-024-01750-9.

[23] Ghafar, W.A.; Zhong, T.; Lai, Z.; Zhang, P.; Yang, Y.; Hasan, M.M. (2025). Seismic isolation for existing structures: A review of retrofitting techniques, case studies, and trends. *Discover Civil Engineering*, *2*, 137. https://doi.org/10.1007/s44290-025-00300-1.

[24] Badan Standardisasi Nasional. (2019). SNI 1726:2019: Tata Cara Perencanaan Ketahanan Gempa untuk Struktur Bangunan Gedung dan Nongedung; Badan Standardisasi Nasional: Jakarta, Indonesia.

[25] Aplikasi Spektrum Respons Desain Indonesia. (accessed on 15 October 2026) Available online: https://rsa.ciptakarya.pu.go.id/2021/.

© 2026 by the authors. This article is an open access article distributed under the terms and conditions of the Creative Commons Attribution (CC BY) license (http://creativecommons.org/licenses/by/4.0/).